Supramolecular Structures of Amyloid-Related Peptides in an Ambient Water Nanofilm

Ming Ye,[†,‡] Yi Zhang,*[,†] Hai Li,[†] Muyun Xie,[†,‡] and Jun Hu[†]

Shanghai Institute of Applied Physics, Chinese Academy of Sciences, Shanghai 201800, China and Graduate School of the Chinese Academy of Sciences, Beijing 100049, China

Received: June 15, 2010; Revised Manuscript Received: September 2, 2010

An ambient water nanofilm condensed on a solid surface provides a good model system to study the self-assembling behaviors of peptides in a confined environment. In this paper, the self-assembly of three short amyloid-related peptides in a water nanofilm confined on a mica substrate was studied using drying microcontact printing (D-μCP) and atomic force microscopy (AFM). The three peptides, which share the same amino acid sequence but have different terminal groups, were placed on mica surfaces by D-μCP. The samples were then incubated in a chamber with a controlled temperature and relative humidity (RH) in which water nanofilms were generated on the sample surfaces. AFM images revealed that the peptides assembled into two kinds of supramolecular structures: nanofilaments and nanosheets. The peptides' terminal groups and the thickness of the water nanofilms determined the self-assembled supramolecular structures in the water nanofilm. Through AFM investigation of the formation and transformation of the peptides' supramolecular structures, we conclude that the peptides' self-assembly process was dominated by weak interactions, such as hydrophobic and electrostatic interactions and hydrogen bonding, between the peptide molecules, the mica substrate, and the water nanofilm. On the basis of these results, a model that describes the peptide arrangement in the confined water nanofilm is proposed. This study reveals the complicated interactions of the peptides at an interface, which may be a general mechanism in vivo because water confinement around biomolecules and membranes is a universal phenomenon.

1. Introduction

The self-assembly of short amyloid-related peptides provides a good model system for an in vitro investigation of the mechanism of a group of diseases, the so-called amyloid diseases, which have been found to be a result of the aggregation and deposition of elongated, unbranched fibrils by misfolded proteins.[1−9] Because the driving forces for the aggregation of those peptides or proteins are normally weak, noncovalent interactions, including hydrogen bonding, van der Waals forces, electrostatic interactions, hydrophobic interaction, and stacking effects,[2,3,10−16] the self-assembly of these peptides often occurs only under certain conditions and is very sensitive to environmental alteration.[17−21] Therefore, although much progress has been made through in vitro investigation, evidence suggests that amyloid formation in vivo is quite different from what happens in a dilute aqueous solution.[22−30]

The different amyloid behaviors in vivo may be induced by the interactions between the amyloid peptides with membranes and the extracellular matrix[31−40] because amyloid formation takes place in a heterogeneous and complicated environment. Indeed, investigations on micelle and membrane systems using NMR and other technologies have confirmed that the structural transformation of amyloid-related peptides is controlled by membrane interfaces and environmental factors.[20,41−44] These structural transformations may be partly responsible for the mechanism of amyloid formation in vivo. In addition, it has been suggested that a crowding environment can have a severe impact on the structural behavior of peptides interacting with membrane interfaces, resulting in the acceleration of peptide aggregation.[40]

We propose that the different properties of water in vivo from in vitro could be another origin for the above-mentioned differences in amyloid formation. The in vivo environment is extremely crowded, containing macromolecules typically separated by only 1−2 nm[45] and surrounded by confined water layers.[46,47] This narrow confinement would be expected to alter the structure, physicochemical properties, and biological function of the water layers. In fact, it has been suggested that the water layers confined at the surfaces of biomolecules in vivo play an important role in biological processes.[45,48,49] Because the direct in vivo study of the influence of the confined water environment on amyloid aggregation is difficult, it is important to establish simplified model systems to understand the relationship between behaviors under in vitro conditions and the real processes in an in vivo confined environment.

In our previous study, we demonstrated that a water nanofilm condensed on a mica surface can be a new model system to investigate the self-assembly behavior of short amyloid-related peptides in a confined water environment.[50] Such water nanofilms have also been used by other scientists to study many important physical and biological processes in many different areas of research.[50−54] We demonstrated that the self-assembly of amyloid-related peptides is sensitive to the amount of water on the solid surfaces, and different peptides with varied molecular structures exhibit different behaviors in the water nanofilms. However, how the peptide self-assembles into supramolecular structures through interactions between the peptides, the water nanofilm, and the substrate is still unclear. This kind of information is very important, as it is a key to mimicking the assembly of amyloid-related peptide in vivo. Further, this assembly may be a general mechanism because

* To whom correspondence should be addressed. Phone: 86-21-39194607. Fax: 86-21-59552394. E-mail: zhangyi@sinap.ac.cn.
† Shanghai Institute of Applied Physics, Chinese Academy of Sciences.
‡ Graduate School of the Chinese Academy of Sciences.

10.1021/jp105501x
Published on Web 11/15/2010

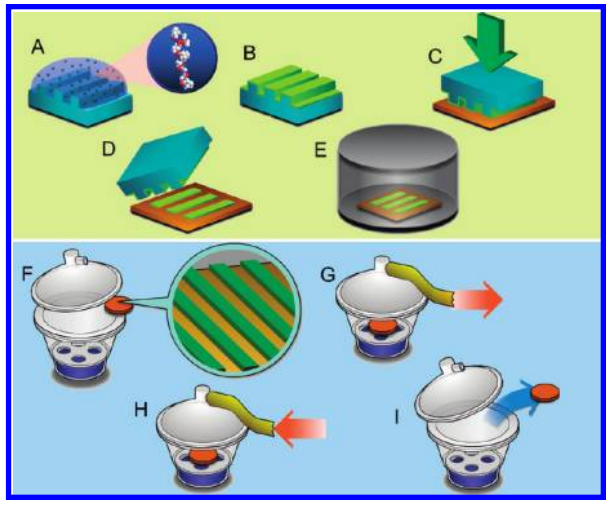

Figure 1. (A−E) Peptide sample preparation process using the μCP method and the water nanofilm treatment. (F−I) Process flow of the generation of supersaturated water vapor using the wet vacuum process.

water confinement around biomolecules and membranes is a universal phenomenon in vivo.

In this paper, we used three short amyloid-related peptides that have the same amino acid sequence but different terminal groups to study the function of noncovalent interactions on the self-assembly of peptides in a confined water system. Two kinds of supramolecular structures, nanofilaments and nanosheets, were found under different water environmental conditions. The factors that dominate the formation and transformation of the peptides' supramolecular structures were systematically investigated. A self-assembly model that describes the peptide arrangement in the confined water nanofilm was proposed based on the experimental results. This study provides new insight into the influences of a confined water environment on the formation and stability of the common amyloid 'steric zipper' structures, which have been found to be the fundamental unit of amyloid-like fibrils, and are important for the investigation of amyloid diseases at the molecular level.[55]

2. Experimental Section

Materials. The peptides GAV9 (NH_2-VGGAVVAGV-$CONH_2$), GAV9a (CH_3CONH-VGGAVVAGV-$CONH_2$), and GAV9b (NH_2-VGGAVVAGV-COOH) were synthesized using the Boc solid-phase method on an ABI 433 A peptide synthesizer (Applied Biosystems) and cleaved from the MBHA resin (100−200 mesh, Fluka) with hydrogen fluoride. The peptides were purified through a TSK-40 (S) column (2.0 cm $\times$98 cm, Tosoh). Before use, the peptides were dissolved in Milli-Q water to a final concentration of 1 mg/mL.

Peptide Patterning. The peptides GAV9, GAV9a, and GAV9b were transported onto a freshly cleaved mica substrate with polydimethylsiloxane (PDMS) stamps using drying microcontact printing (D-μCP) technology. A detailed description of this process can be found in our previous paper.[50] In brief, a PDMS stamp was first inked with a peptide aqueous solution and dried with nitrogen flow (Figure 1A−C). Then, strip-like peptide patterns (Figure 1D and 2A) were formed by pressing the inked PDMS stamp onto the mica substrate. All of the peptide patterns on the substrate surfaces had a strip width of

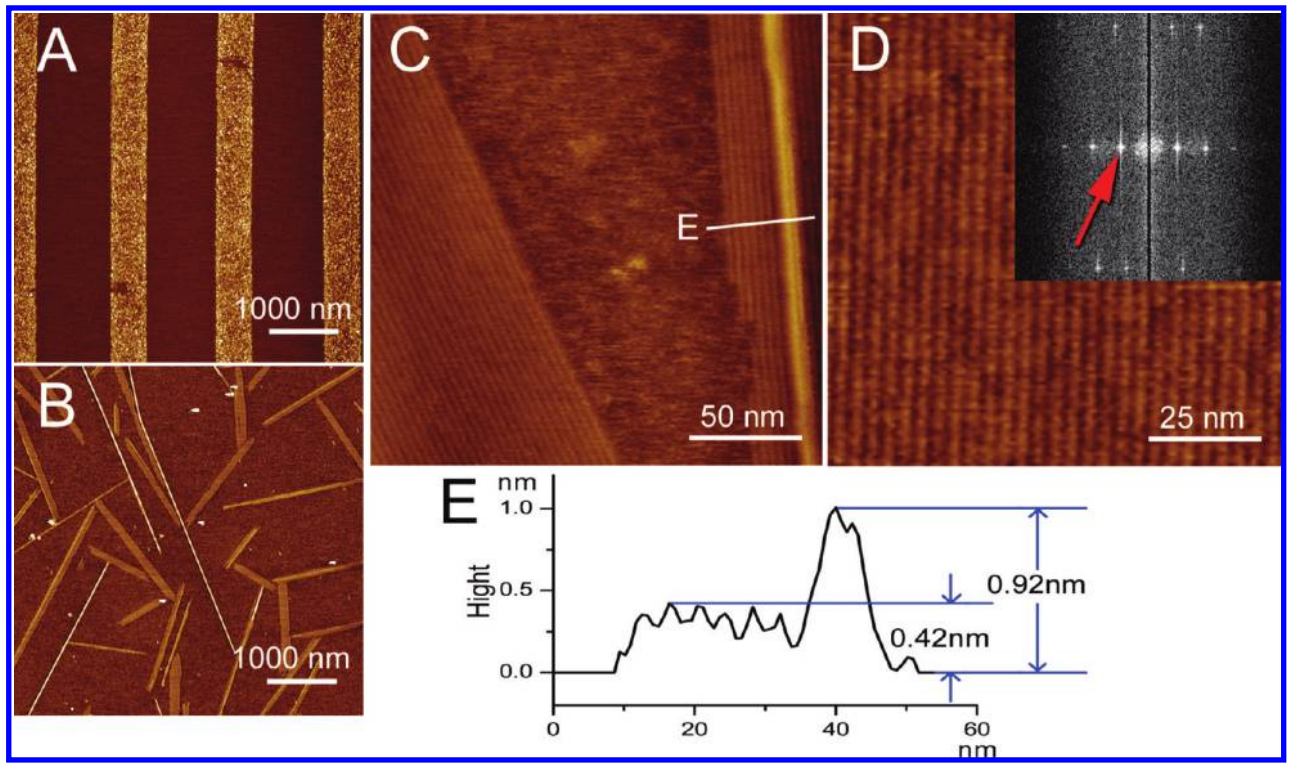

Figure 2. AFM observation of the two kinds of self-assembling structures of the GAV9a peptide generated in 100% RH condition. (A) Peptides transport on mica surface by the D-μCP method. (B) GAV9a peptide has self-assembled in two kinds of aggregation structures after 20 h in a water nanofilm environment. (C) High-resolution image of the aggregation structures showing the detailed structure of both kinds of peptide aggregation structures. (D) Detail of the lower nanosheet structure. The light regions represent the backbones of peptides, while the dark regions are the gaps between two linear units. (Inset in D) Two-dimensional Fourier transform of part D, where the average lateral spacing between the single nanofilaments in the nanosheet structure, determined from the radial position of spots (red arrow) in the Fourier transform patterns of images, was equal to 3.6 $\pm$ 0.2 nm. (E) Section analysis of line E in part C. The height of the nanofilament structure is ~0.92 nm, and that of the nanosheet structure is ~0.42 nm.

TABLE 1: Aggregation Structures of Three Kinds of Peptides under Different Humidity Conditions

peptide	terminal group	RH (%)	self-assembling structure
GAV9	N-terminus: NH_2- C-terminus, $-CONH_2$	40	slow diffusion, no structure
		70	nanofilament
		100	nanofilament
GAV9a	N-terminus: CH_3CONH- C-terminus, $-CONH_2$	40	nanofilament
		70	nanofilament
		100	nanosheet/nanofilament
GAV9b	N-terminus, NH_2-; C-terminus, $-COOH$	40	slow diffusion, no structure
		70	nanosheet
		100	nanosheet

0.5 μm and a period of 1.6 μm, with the thickness of the strips varying between 0.5 and 1.5 nm. The D-μCP process was conducted at room temperature and with a relative humidity (RH) of ~40% or less.

Formation of Ambient Water Nanofilm on Mica and Incubation of Samples. A sample chamber (SDH-01N, Shanghai Jianheng Instrument Co.) was used in which the RH and temperature was controlled with an accuracy of 5% and 0.1 °C, respectively. The samples with patterned peptides were incubated in the chamber for a given amount of time (Figure 1E). At room temperature, condensed water nanofilms formed on the bare mica substrate between the peptide strips at elevated RH. The thickness of the water nanofilm was adjusted by the RH in the range of 30−100% within the chamber. During incubation, the peptide on the strips diffused and self-assembled into different structures in the water nanofilm.[50]

Atomic Force Microscope (AFM) Observation. An AFM (Multimode Nanoscope IIIa, Vecco/Digital Instruments, Santa Barbara, CA) equipped with a J scanner (100 μm × 100 μm) and an E scanner (15 μm × 15 μm) was employed to reveal the self-assembled peptide supramolecular structures. Commercially available silicon cantilevers with a nominated force constant of ~48 N/m and a resonant frequency of ~330 kHz (NSC11, MikroMasch Co.) or with a nominated force constant of ~11.5 N/m and a resonant frequency of ~255 kHz (NSG11, NT-MDT Co., Russia) were used. All AFM operations were carried out in air at room temperature with a RH of 40%.

Sample Treatment with Supersaturated Water Vapor. To generate supersaturated water vapor conditions for forming thicker water nanofilms on the mica substrates, we used a method called the "wet vacuum process". A glass vacuum vessel and liquid ring pump were used in this step. The volume of the vessel was 4150 mL. First, 600 mL of pure water was infused into the vessel, and mica samples with peptides strips were placed on a clapboard within the vessel (Figure 1F). Then, the pressure in the vessel was reduced with the liquid ring pump to about 4 kPa, which is a little higher than the saturated water vapor pressure at a temperature of 293 K (Figure 1G). When the inner pressure was maintained at 4 kPa, the water in the vessel evaporated to preserve this pressure. After 5 min, the valve between the vessel and the pump was closed and the vacuum pump was removed. The valve on the vessel was then linked to the environmental atmosphere to allow air (~50% RH) to enter the vessel with a controlled flow rate of ~90 mL/s (Figure 1H). During this process, a supersaturated water vapor condition was generated in the vessel in a short time. When the pressure was equilibrated between the inside and the outside of the vessel, the samples were taken from the vessel and transferred immediately into a sealed box which was half-filled with dry silica gel (Figure 1I).

3. Results and Discussion

Water nanofilm on mica surface is a well-studied model for confined water systems.[54,56] The structure and thickness of the water nanofilms can be adjusted by environmental RH and temperature. At room temperature, the first fully covered water monolayer on the mica surface appears at 70% RH with a thickness around 0.3 nm, which increases to several nanometers when the water vapor in the environment is saturated.[57] Under saturated water vapor conditions, the water nanofilm is thick enough to generate a bulk-like hydrophobic vapor/water interface.[58]

We used three short peptides, which originate from a conserved consensus of several neurodegenerative disease-related proteins such as α-synuclein, β-amyloid protein, and prion protein.[18,59] The peptides, named GAV9, GAV9a, and GAV9b, respectively, share the same amino acid sequence (VGGAVVAGV) but have different terminal groups (Table 1). After the peptides were transferred onto freshly cleaved mica surfaces with patterned microstrips (Figure 2A), a humidity- and temperature-controlled environment was created to form a water nanofilm on the surfaces. The peptides then diffused on the surface and self-assembled into 1-D epitaxial nanostructures under well-controlled conditions.[50] Subsequent AFM observations indicated that the peptides responded differently according to the environment RH.

In our previous work, we studied the behaviors of several peptides in the water nanofilm environment. We generally call all the self-assembled peptide nanostructures "nanofilaments".[50] However, after comparing the assembled supramolecular structures between the three peptides studied in this paper, we found that such nanostructures are actually composed by two different forms. One type of supramolecular structure is composed of individual, separated nanofilaments, while the other is in a nanosheet shape (Figure 2B). In the case of nonpolar GAV9a peptide, these two kinds of supramolecular structures can coexist under certain conditions. The high-resolution AFM image shown in Figure 2C provides more details of these coexisting structures. Both of the supramolecular structures are formed by small linear units with the same apparent width. However, the nanosheet structures are usually formed by units with a height of ~0.42 nm, while the nanofilaments are formed by linear units with a height of ~0.92 nm, almost twice the height of the former units (Figure 2E).

On the other hand, we found that the three peptides respond differently to environmental conditions (Table 1), although they only differ in their terminal groups. By controlling RH at room temperature, GAV9a with an amide group at the C-terminus and an acetamide group at the N-terminus could self-assemble into either nanofilaments or nanosheets (Figure 3B) on the mica substrate. However, at all RHs we studied, the GAV9 with an amide group at the C-terminus and an amino group at the N-terminus only self-assembled into nanofilaments (Figure 3A), while the GAV9b with a carboxyl group at the C-terminus and an amino group at the N-terminus only formed nanosheets (Figure 3C). Notably, the GAV9a molecules could diffuse on the substrate and self-assemble at a low humidity (e.g., 40%

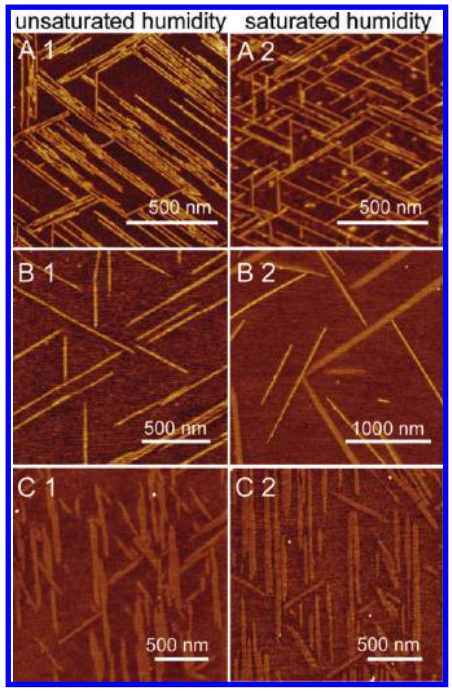

Figure 3. (A) For the GAV9, only nanofilament structure formed at 20 °C, 70% RH (A1) and 20 °C, 100% RH (A2). (B) For the GAV9a, only nanofilament structure formed at 20 °C, 70% RH (B1) but at 20 °C, 100% RH both nanofilament and nanosheet structures formed (B2). (C) For the GAV9b, only nanosheet structure formed at 20 °C, 70% RH (C1) and 20 °C, 100% RH (C2).

RH); however, under these RHs, the other two peptides could only diffuse on the substrate and not self-assemble into regular structures.

From the two-dimensional Fourier transforms of Figure 2D, the averaged lateral spacing between the linear units of the nanosheet features is 3.6 ± 0.2 nm (red arrow in the inset of Figure 2D). The lateral spacing between the basic linear units in the nanofilaments (3.4 ± 0.4 nm) is similar to that of the nanosheets. In comparison, the theoretical length of a fully extended 9-residue peptide in a β-sheet conformation[60] is ~3.3 nm. Because our previous ATR-IR study indicated that the GAV9 forms antiparallel β-sheet structures on mica surfaces,[50] the above result suggests that the 3.6 nm wide linear units are formed by peptide chains perpendicular to the long axis of the basic linear units with a β-sheet conformation. The parameters of a crystal cell of Muscovite mica we used were $a = 0.519$ nm and $b = 0.904$ nm. The length of the single GAV9a peptide chain is close to 4 times the length of parameter b of the mica lattice (3.616 nm).

The above result suggests that the basic linear unit for both nanofilament and nanosheet structures is formed by peptides with a β-sheet conformation. However, the basic linear unit in the nanosheet structure is formed only by a single layer of peptides. This kind of structure is usually found in the aggregations of amyloid peptides on hydrophobic substrates.[18,61] In contrast, the linear unit in the higher nanofilament is formed by two peptide layers (Figure 4A). The two peptide layers could form a "dry steric zipper" structure between their side chains.[55] Such structure would protect the hydrophobic side chains of peptide molecules from the surrounding water molecules and has been found in the cores of many misfolded proteins, which are composed of very different sequences but all are in a pair of β-sheet conformations.[55,62−65]

The different responses of the three GAV9 peptides to the various environmental RHs shed light on the complicated interactions between peptides, substrate, and the water nanofilm. It is clear that electrostatic interactions, hydrophobic interactions, hydrogen bonds, and the effects of confined water layers should be taken into account in the peptide self-assembly process. The three peptides are composed of hydrophobic amino residuals; therefore, the hydrophobic interactions between the peptide molecules are strong, which provides a driving force for their self-assembly. The hydrogen bonds between the peptide molecules also facilitate the formation of the basic linear units. In addition, the electrostatic interaction between the charged peptides (GAV9 and GAV9b) and the mica substrate modulates the self-assembly process and might be one of the important origins for the epitaxial arrangement of the nanofilaments and nanosheets. The angle between basic linear units on cleaved mica equals 120°. This phenomenon is similar to the ordered water islands formed on mica,[52,66] which has been related to the ordering of hydrated K^+ ions on the mica surface.[67] We think that the hydrated K^+ ions on cleaved mica may also influence the assembly of the GAV9 and GAV9b peptides with an analogous manner. Furthermore, the hydrophobic peptides may also interact with a hydrophobic bulk-like vapor/water interface generated in the water nanofilm on a substrate at high RHs. Our previous results indicate that supramolecular structures

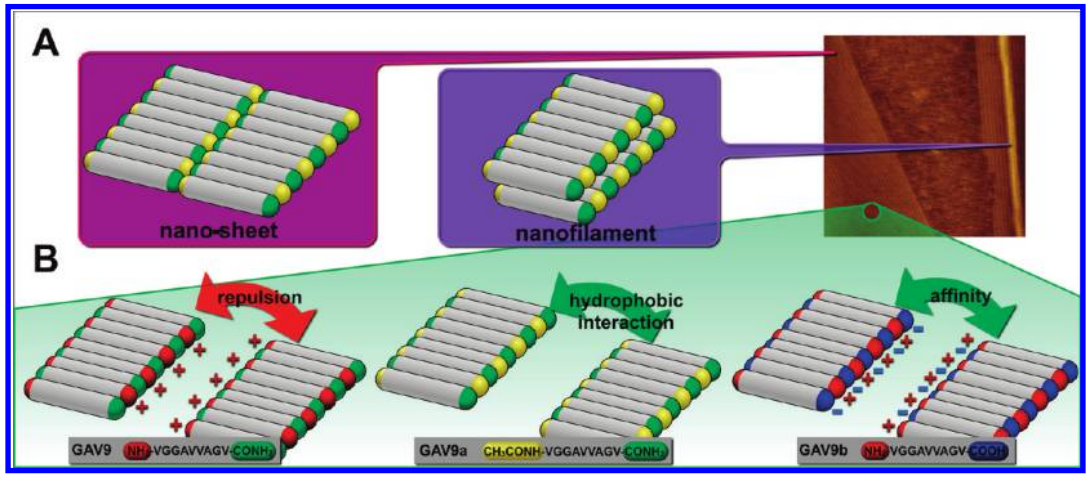

Figure 4. Schematic representation of (A) the model of two different structures of GAV9/GAV9a/GAV9b peptides formed in a water nanofilm. (B) Roles of terminal groups and hydrophobic interaction in the appearance of two structures under different conditions. The single peptide molecule is shown as a gray stick with different colored terminal groups.

of peptides formed in water nanofilm and in bulk water on mica are quite different,[50] which is strong evidence for the influence of the vapor/water interface on the self-assembly of peptides in the water nanofilm. The vapor/water interface has been studied previously by X-ray reflectivity measurements and molecular simulation.[10,58] This kind of hydrophobic interaction that results in accumulation and conformational changes of peptides at the vapor/water interface has been reported.[32]

The apparent heights of the nanofilaments (~0.92 nm) and nanosheets (~0.42 nm) formed at 100% RH is much smaller than the thickness of water nanofilms adsorbed on cleaved mica at this RH, which was reported previously to be about 2−3 nm.[68,69] Therefore, how the flat lying supramolecular structures were formed by the interaction of the peptides with the vapor/water interface is interesting. We think that the "tilting" models of the amphiphilic surfactants on cleaved mica are helpful to explain our results.[67,70,71] Since the peptide molecules have a length of ~3 nm, the peptide may take a "tilting" orientation so that the molecule can partly interact with both the substrate and the vapor/water interface. The peptides in the water nanofilms with different thicknesses may also have different tilting degrees. When the RH decreased to <40% for AFM observation, the peptides would lie flat on the mica substrate.

The GAV9 molecule is positively charged at its N-terminus and is nonpolar at its C-terminus. If it formed a nanosheet structure with an antiparallel β-sheet conformation, both sides of a linear unit in the nanosheet structure would be positive charged, and the repulsive electrostatic force between linear units would make the nanosheet structure unstable (Figure 4B). Therefore, it is hard to form sheet structures. In contrast, the GAV9b molecule has oppositely charged terminal groups at its ends. In an antiparallel β-sheet structure formed with GAV9b, the linear unit will have alternately negative/positive charges at both of its sides (Figure 4B). So the electrostatic attraction between linear units can stabilize the sheet structure.

For the nonpolar GAV9a, the hydrophobic interactions between the side chains of the peptides play an important role during self-assembly in the water nanofilm generated on mica under lower RH conditions. In this case, only two-layer nanofilaments were observed. When the RH is close to 100%, the assembly of GAV9a is affected by the formation of a hydrophobic vapor/water interface and the strong hydrophobic interaction between GAV9a side chains with the vapor/water interface would take effect. Therefore, most GAV9a peptides tend to extend their side chains to the vapor/water interface to form a single-layer nanosheet structure. In contrast to GAV9 and GAV9b, there is no electrostatic interaction between the GAV9a and the substrate. The epitaxy of its supramolecular structures on the substrate can be interpreted as a joint result of the geometrical lattice matching and the limited possible orientations of the peptide molecules in the confined water nanofilm. The geometrical lattice matching and water confinement effects may also be responsible for our previous finding that GAV9a shows very different epitaxial orientations under different RHs,[50] in which it forms epitaxial nanofilaments at RH $\approx$ 55−70%, but the epitaxial orientation began to shift at higher RH.

Interestingly, the nanofilaments do not expand laterally and form two-layer films. One reasonable explanation for this result is that the formation of the upper layer depends on the orientations of the linear units in the bottom layer on the 2-D substrate. Because the peptide molecules form an antiparallel β-sheet structure, one linear unit in the bottom layer of the nanofilaments could take two enantiomorphous orientations in one lattice direction of the mica substrate. If two nearby linear units take opposite orientations, then their upper layers could not coexist because of the steric hindrance.[55] Because GAV9a has nonpolar groups at both ends, two nearby linear units in the bottom layer are free to take the same or opposite orientations, each with a 50% probability. Therefore, the probability of forming a two-layer nanofilament with n linear units could be expressed as $1/2^{n-1}$ if one ignores the kinetic difference between the two aggregation processes.

Peptides Self-Assembly on a Mica Substrate in a Supersaturated Water Vapor Environment. To further study the role of the substrates in these peptides self-assembling processes, we designed a new experimental method we called the "wet vacuum process", which generates a much thicker water film on the mica substrate by taking advantage of a supersaturated water vapor environment. Using this method, it is now possible to provide a water film that is thick enough for the peptides to generate aggregate structures that were influenced by substrates weakly.

This wet vacuum process takes advantage of the principle that the saturated water vapor pressure in air is a function of temperature and independent of environment pressure. In step G in Figure 1, the pressure in the vacuum vessel was around 4 kPa and the saturated vapor pressure of water under those conditions is 2.31 kPa. Therefore, most of the gas phase in the vessel was water vapor and the RH was around 100%. In step H, 50% RH air was refilled into the vacuum vessel, which led the water vapor in the vacuum vessel to become supersaturated. At this moment, more water was condensed on the surface of mica substrate than 100% RH condition and formed a much thicker water nanofilm. Although such a state is not stable and cannot last long enough for a quantifiable measurement, the peptides with hydrophobic side chains could assemble more freely on the water film because of the strong interaction between the peptides and the vapor/water interface. When the pressure in the vacuum vessel became equal to the environment, the humidity in the vessel also returned to the outside RH, which was controlled around 50%, and this resulted in the evaporation of the condensed water over the mica. The peptide supramolecular structures assembled through this process are immobilized on the mica surface.

As a proof-of-concept, we self-assembled GAV9a and GAV9b peptides on mica substrates through the wet vacuum process. We found that the time required for the formation of supramolecular structures for both GAV9a and GAV9b decreased remarkably from tens of hours to several minutes. The acceleration of the peptide assembly process can be possibly attributed to the decrease of the free energy barrier for peptide self-assembly upon an increase of water film thickness under the supersaturated water vapor environment. The GAV9a formed mostly nanosheet structures with occasional nanofilaments on the mica substrate (Figure 5A). The linear units of the nanosheets extended randomly and did not show any epitaxial relation with the underlying mica lattice, which is quite different from those nanostructures formed in 100% RH. The GAV9b formed nanosheet structures similar to GAV9a, although no nanofilaments were observed (Figure 5B). Such results agreed with the hypothesis above that the much thicker water film decreased the influence of the substrate, which resulted in the absence of epitaxy. When we incubated the nanosheet structures under a 100% RH environment, they rearranged and formed supramolecular structures that were epitaxial with the mica lattices. For example, as shown in Figure 5C, some GAV9b sheets were partially arranged (blue arrow) while the others maintained

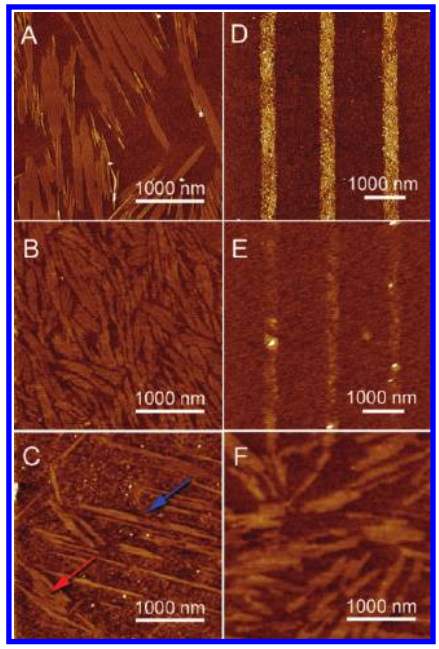

Figure 5. AFM images of peptide structures after the wet vacuum process on different substrates. (A) GAV9a nanosheet and nanofilament structure on the mica substrate after the wet vacuum process. (B) GAV9b nanosheet structures on the mica substrate after the wet vacuum process. (C) When the sample in B was transported into a 100% RH environment for 2 h, the nanosheet structure partly reformed to fit the orientation of the mica substrate (blue arrow). (D) D-μCP generated GAV9a strips on a silicon oxide surface. (E) After incubating the sample in D in a 100% RH and 20 °C environment for 20 h, only diffusion of the peptides could be observed. (F) On treating the sample in D with the wet vacuum process, nanosheet structures could be observed on the silicon oxide surface.

random orientations (red arrow) after incubation under an environment of 100% RH and 20 °C for 2 h. When the incubation time is long enough, the sheets almost all rearranged.

In addition, we used a naturally oxidized hydrophilic silicon (111) substrate as a control. It has been reported that under high RH, the silicon oxide surface also forms water nanofilms above it that have a thickness similar to that on a mica substrate.[72] The main difference of such substrate from the mica substrate is the lacking of a periodic lattice structure like mica. On the silicon oxide surface, normal humidity conditions were tested (Figure 5D and 5E). Only the diffusion of peptide molecules and no assembled supramolecular structures could be observed on this substrate. However, after using the wet vacuum process, nanosheet structures similar to those found on the mica surface were also observed (Figure 5F).

In a bulk aqueous solution without a substrate, the GAV9 peptides only form random-coil aggregates,[18] which is quite different than the structures reported here. Therefore, under the supersaturated water vapor condition, the substrate still has its influence on the peptide self-assembly. However, the supramolecular structures self-assembled from GAV9a and GAV9b peptides lost ordered orientation along the underneath mica lattice, which suggests that the substrate has less influence on the formation of these nanosheet structures than in normal water nanofilm. Under such conditions, the hydrophobic vapor/water interface would play a more important role on the assembly of the peptides. When the supersaturated water vapor restores to normal environmental RH, the influence of substrate dominates again.

4. Conclusion

In summary, we studied the self-assembly of three short GAV9 peptides in a confined water environment on a solid substrate. We investigated the roles of peptide terminal groups, the environmental RHs, and the confinement effect of water nanofilms on the peptides' supramolecular structure formation. Two kinds of assembled supramolecular structures were found: two-layer nanofilaments and one-layer nanosheets. Moreover, we observed a transformation between these two supramolecular structures under different RH conditions for GAV9a peptide. A model that describes the self-assembling behaviors of the peptides in the water nanofilm confined on the substrate was suggested. Our results clearly indicate that a confined water nanofilm could strongly influence the self-assembly process of amyloid-related peptides. Since confinement of water layers on biomembranes and biomolecules is universal,[45,73] these findings suggest that the roles of the confined water should not be ignored when investigating amyloid formation in vivo. In addition, this study provides a potential method for fabricating structure-controlled nanomaterials by self-assembly of functional-group-tailored peptides at the solid interfaces.

Acknowledgment. This work was partly supported by grants from Chinese Academy of Sciences (Nos. KJCX2.YW.H06 and KJCX2.YW.M03), the National Science Foundation of China (Nos. 10975175 and 90923002), the National Basic Research Program of China (No. 2007CB936000), the Ministry of Health of China (2009ZX10004-301), and the Science and Technology Commission of Shanghai Municipality (0952 nm04600).

References and Notes

(1) Dobson, C. M. *Nature* **2003**, *426*, 884.
(2) Chiti, F.; Calamai, M.; Taddei, N.; Stefani, M.; Ramponi, G.; Dobson, C. M. *Proc. Natl. Acad. Sci. U.S.A.* **2002**, *99*, 16419.
(3) Otzen, D. E.; Kristensen, O.; Oliveberg, M. *Proc. Natl. Acad. Sci. U.S.A.* **2000**, *97*, 9907.
(4) Selkoe, D. J. *Nature* **2003**, *426*, 900.
(5) Deng, M.; Yu, D.; Hou, Y.; Wang, Y. *J. Phys. Chem. B* **2009**, *113*, 8539.
(6) Xu, S. *J. Phys. Chem. B* **2009**, *113*, 12447.
(7) Barrow, C. J.; Zagorski, M. G. *Science* **1991**, *253*, 179.
(8) Harper, J. D.; Wong, S. S.; Lieber, C. M.; Lansbury, P. T. *Biochemistry* **1999**, *38*, 8972.
(9) Nguyen, K. T.; King, J. T.; Chen, Z. *J. Phys. Chem. B* **201**, *114*, 8291.
(10) Pratt, L. R.; Pohorille, A. *Chem. Rev.* **2002**, *102*, 2671.
(11) Chatani, E.; Kihara, M.; Ban, T.; Sakai, M.; Hasegawa, K.; Naiki, H.; Rao, C. M.; Goto, Y. *Biochemistry* **2005**, *44*, 1288.
(12) Taddei, N.; Stefani, M.; Ramponi, G.; Chiti, F. *Biochemistry* **2003**, *42*, 15078.
(13) Schmittschmitt, J. P.; Scholtz, J. M. *Protein Sci.* **2003**, *12*, 2374.
(14) Zurdo, J.; Guijarro, J. I.; Jimez, J. L.; Saibil, H. R.; Dobson, C. M. *J. Mol. Biol.* **2001**, *311*, 325.
(15) Tjernberg, L.; Hosia, W.; Bark, N.; Thyberg, J.; Johansson, J. *J. Biol. Chem.* **2002**, *277*, 43243.
(16) Kim, W.; Hecht, M. H. *Proc. Natl. Acad. Sci. U.S.A.* **2006**, *103*, 15824.
(17) Whitesides, G. M.; Grzybowski, B. *Science* **2002**, *295*, 2418.
(18) Zhang, F.; Zhang, Z.-X.; Ji, L.-N.; Li, H.-T.; Tang, L.; Wang, H.-B.; Fan, Ch.-H.; Xu, H.-J.; Zhang, Y.; Hu, J.; Hu, H.-Y.; He, J.-H, *Angew. Chem., Int. Ed.* **2006**, *45*, 3611.
(19) Shen, C. L.; Murphy, R. M. *Biophys. J.* **1995**, *69*, 640.
(20) Marcinowski, K. J.; Shao, H.; Clancy, E. L.; Zagorski, M. G. *J. Am. Chem. Soc.* **1998**, *120*, 11082.
(21) Castelletto, V.; Hamley, I. W.; Cenker, C.; Olsson, U. *J. Phys. Chem. B* **2010**, *114*, 8002.
(22) Sabate, R.; Estelrich, J. *J. Phys. Chem. B* **2005**, *109*, 11027.
(23) Scheuner, D.; Eckman, C.; Jensen, M.; Song, X.; Citron, M.; Suzuki, N.; Bird, T. D.; Hardy, J.; Hutton, M.; Kukull, W.; Larson, E.; Levy-Lahad, L.; Viitanen, M.; Peskind, E.; Poorkaj, P.; Schellenberg, G.; Tanzi, R.; Wasco, W.; Lannfelt, L.; Selkoe, D.; Younkin, S. *Nat. Med.* **1996**, *2*, 864.
(24) Wang, R.; Sweeney, D.; Gandy, S. E.; Sisodia, S. S. *J. Biol. Chem.* **1996**, *271*, 31894.

(25) Lewczuk, P.; Esselmann, H.; Groemer, T. W.; Bibl, M.; Maler, J. M.; Steinacker, P.; Otto, M.; Kornhuber, J. Wiltfang. *J. Biol. Psych.* **2004**, *55*, 524.
(26) Yamagata, S. K.; Jr., C. L. E.; Higson, G. J.; Neynaber, S. A.; Parson, R. E.; Munroe, W. A. *J. Neurochem.* **1996**, *66*, 259.
(27) Haass, C.; Schlossmacher, M. G.; Hung, A. Y.; Vigo-Pelfrey, C.; Mellon, A.; Ostaszewski, B. L.; Lieberburg, I.; Koo, E. H.; Schenk, D.; Teplow, D. B.; Selkoe, D. J. *Nature* **1992**, *359*, 322.
(28) Shoji, M.; Golde, T.; Ghiso, J.; Cheung, T.; Estus, S.; Shaffer, L.; Cai, X.; McKay, D.; Tintner, R.; Frangione, B. *Science* **1992**, *258*, 126.
(29) Seubert, P.; Vigo-Pelfrey, C.; Esch, F.; Lee, M.; Dovey, H.; Davis, D.; Sinha, S.; Schiossmacher, M.; Whaley, J.; Swindlehurst, C.; McCormack, R.; Wolfert, R.; Selkoe, D.; Lieberburg, I.; Schenk, D. *Nature* **1992**, *359*, 325.
(30) Andisheh, A.; Daniel, P. R. *Phys. Biol.* **2009**, *6*, 015005.
(31) Snow, A. D.; Wight, T. N. *Neurobiol. Aging* **1989**, *10*, 481.
(32) Jiang, D.; Dinh, K. L.; Ruthenburg, T. C.; Zhang, Y.; Su, L.; Land, D. P.; Zhou, F. *J. Phys. Chem. B* **2009**, *113*, 3160.
(33) Quist, A.; Doudevski, I.; Lin, H.; Azimova, R.; Ng, D.; Frangione, B.; Kagan, B.; Ghiso, J.; Lal, R. *Proc. Natl. Acad. Sci. U.S.A.* **2005**, *102*, 10427.
(34) Knight, J. D.; Miranker, A. D. *J. Mol. Biol.* **2004**, *341*, 1175.
(35) Munishkina, L. A.; Fink, A. L. *Biomembranes* **2007**, *1768*, 1862.
(36) Inoue, S. *Int. Rev. Cytol.* **2001**, *210*, 121.
(37) Ancsin, J. B. *Amyloid* **2003**, *10*, 67.
(38) Lashuel, H. A.; Lansbury, P. T. *Q. Rev. Biophys.* **2006**, *39*, 167.
(39) Sipe, J. D.; Cohen, A. S. *Crit. Rev. Clin. Lab. Sci.* **1994**, *31*, 325.
(40) Bokvist, M.; Gröbner, G. *J. Am. Chem. Soc.* **2007**, *129*, 14848.
(41) Coles, M.; Bicknell, W.; Watson, A. A.; Fairlie, D. P.; Craik, D. J. *Biochemistry* **1998**, *37*, 11064.
(42) Shao, H.; Jao, S.-c.; Ma, K.; Zagorski, M. G. *J. Mol. Biol.* **1999**, *285*, 755.
(43) Terzi, E.; Holzemann, G.; Seelig, J. *Biochemistry* **1997**, *36*, 14845.
(44) Yip, C. M.; Darabie, A. A.; McLaurin, J. *J. Mol. Biol.* **2002**, *318*, 97.
(45) Ball, P. *Chem. Rev.* **2008**, *108*, 74.
(46) Teschke, O.; de Souza, E. F. *Chem. Phys. Lett.* **2005**, *403*, 95.
(47) Cherepanov, D. A.; Feniouk, B. A.; Junge, W.; Mulkidjanian, A. Y. *Biophys. J.* **2003**, *85*, 1307.
(48) Chaplin, M. *Na.t Rev. Mol. Cell. Biol.* **2006**, *7*, 861.
(49) Gawrisch, K.; Ruston, D.; Zimmerberg, J.; Parsegian, V. A.; Rand, R. P.; Fuller, N. *Biophys. J.* **1992**, *61*, 1213.
(50) Li, H.; Zhang, F.; Zhang, Y.; Ye, M.; Zhou, B.; Tang, Y.-Z.; Yang, H.-J.; Xie, M.-Y.; Chen, S.-F.; He, J.-H.; Fang, H.-P.; Hu, J. *J. Phys. Chem. B* **2009**, *113*, 8795.
(51) Zhu, Y.; Granick, S. *Phys. Rev. Lett.* **2001**, *87*, 096104.
(52) Xu, L.; Lio, A.; Hu, J.; Ogletree, D. F.; Salmeron, M. *J. Phys. Chem. B* **1998**, *102*, 540.
(53) Park, C.; Fenter, P. A.; Nagy, K. L.; Sturchio, N. C. *Phys. Rev. Lett.* **2006**, *97*, 016101.
(54) Verdaguer, A.; Sacha, G. M.; Bluhm, H.; Salmeron, M. *Chem. Rev.* **2006**, *106*, 1478.
(55) Sawaya, M. R.; Sambashivan, S.; Nelson, R.; Ivanova, M. I.; Sievers, S. A.; Apostol, M. I.; Thompson, M. J.; Balbirnie, M.; Wiltzius, J. J. W.; McFarlane, H. T.; Madsen, A. O.; Riekel, C.; Eisenberg, D. *Nature* **2007**, *447*, 453.
(56) Ewing, G. E. *Chem. Rev.* **2006**, *106*, 1511.
(57) Cantrell, W. C.; Ewing, G. E. *J. Phys. Chem. B* **2001**, *105*, 5434.
(58) Wang, J.; Kalinichev, A. G.; Kirkpatrick, R. J.; Cygan, R. T. *J. Phys. Chem. B* **2005**, *109*, 15893.
(59) Du, H.-N.; Tang, L.; Luo, X.-Y.; Li, H.-T.; Hu, J.; Zhou, J.-W.; Hu, H.-Y. *Biochemistry* **2003**, *42*, 8870.
(60) Marsh, R. E.; Corey, R. B.; Pauling, L. *Biochim. Biophys. Acta* **1955**, *16*, 1.
(61) Kowalewski, T.; Holtzman, D. M. *Proc. Natl. Acad. Sci. U.S.A.* **1999**, *96*, 3688.
(62) Astbury, W. T.; Dickinson, S. *Biochem. J.* **1935**, *29*, 2351.
(63) Sunde, M.; Blake, C. *Adv. Protein Chem.* **1997**, *50*, 123.
(64) Eanes, E. D.; Glenner, G. G. *J. Histochem. Cytochem.* **1968**, *16*, 673.
(65) Sunde, M.; Serpell, L. C.; Bartlam, M.; Fraser, P. E.; Pepys, M. B.; Blake, C. C. F. *J. Mol. Biol.* **1997**, *273*, 729.
(66) Hu, J.; Xiao, X.-D.; Ogletree, D. F.; Salmeron, M. *Science* **1995**, *268*, 267.
(67) Meleshyn, A. *J. Phys. Chem. C* **2008**, *112*, 14495.
(68) Beaglehole, D.; Radlinska, E. Z.; Ninham, B. W.; Christenson, H. K. *Phys. Rev. Lett.* **1991**, *66*, 2084.
(69) Cantrell; Ewing, G. E. *J. Phys. Chem. B* **2001**, *105*, 5434.
(70) Mellott, J. M.; Hayes, W. A.; Schwartz, D. K. *Langmuir* **2004**, *20*, 2341.
(71) Benítez, J. J.; Kopta, S.; Díez-Pérez, I.; Sanz, F.; Ogletree, D. F.; Salmeron, M. *Langmuir* **2002**, *19*, 762.
(72) Asay, D. B.; Kim, S. H. *J. Phys. Chem.* **2005**, *109*, 16760.
(73) Pal, S. K.; Zewail, A. H. *Chem. Rev.* **2004**, *104*, 2099.

JP105501X